RSC Publishing Faraday Discussions

Diruthenium Complexes Having a Partially Hydrogenated Bipyridine Ligand: Plausible Mechanism for the Dehydrogenative Coupling of Pyridines at a Diruthenium Site

Journal:	*Faraday Discussions*
Manuscript ID	FD-ART-04-2019-000029.R1
Article Type:	Paper
Date Submitted by the Author:	24-Apr-2019
Complete List of Authors:	Takao, Toshihiro; Tokyo Institute of Technology, Applied Chemistry Kawashima, Takashi; Tokyo Institute of Technology, Applied Chemistry Nagae, Ryo; Tokyo Institute of Technology, Applied Chemistry Kanda, Hideyuki; Tokyo Institute of Technology, Applied Chemistry Watanabe, Wataru; Tokyo Institute of Technology, Applied Chemistry

Journal Name

ARTICLE

Diruthenium Complexes Having a Partially Hydrogenated Bipyridine Ligand: Plausible Mechanism for the Dehydrogenative Coupling of Pyridines at a Diruthenium Site

Received 00th January 20xx,
Accepted 00th January 20xx

DOI: 10.1039/x0xx00000x

www.rsc.org/

Toshiro Takao,* Takashi Kawashima, Ryo Nagae, Hideyuki Kanda, and Wataru Watanabe

Reactions of the diruthenium tetrahydrido complex, Cp*Ru(μ-H)$_4$RuCp* (**1**) (Cp* = η^5-C$_5$Me$_5$), with pyridines were investigated in relation to the dehydrogenative coupling of 4-substituted pyridines. Complex **1** reacted with γ-picoline to yield the bis(μ-pyridyl) complex, {Cp*Ru(μ-H)(μ-4-MeC$_5$H$_3$)}$_2$ (**2a**), with elimination of dihydrogen. Complex **2a** immediately reacted with the liberated dihydrogen to yield μ-η^2-dihydrobipyridine (dhbpy) complex **4a** via C–C bond formation between the two pyridyl groups, in which one of the pyridine rings underwent partial hydrogenation. The X-ray structure of **4a** showed that the dhbpy moiety adopts a μ-η^2 coordination mode at the Ru$_2$ site. Complex **4a** was reversibly converted to **5a** via the elimination of dihydrogen in which the dhbpy moiety adopts a μ-η^2:η^2 mode. Although **5a** was coordinatively saturated, **5a** readily reacted with ^{t}BuNC to yield **6a**. This was owing to the ability of the dhbpy ligand changing its coordination mode between the μ-η^2:η^2 and μ-η^2 modes. This also causes the dehydrogenation from the dhbpy ligand to yield μ-η^2:η^2-bipyridine complex **7a** at 140 °C. However, **7a** was not shown to be an intermediate of the catalysis. The reaction of **1** with 1,10-phenanthroline afforded μ-η^2-phenanthroline complex **8** containing two hydrides, which can be a model compound for the bipyridine eliminationsion from the Ru$_2$ site. Dynamic NMR studies suggested that **8** was isomerised to an unsaturated μ-*N*-heterocyclic carbene (NHC) complex. The unsaturated nature of the μ-NHC complex is likely responsible for the uptake of the third pyridine molecule to turn over the catalytic cycle.

Introduction

The reactivity of multinuclear complexes with pyridine has been intensively studied using carbonyl clusters, and facile formation of a μ-pyridyl ligand on a multimetallic site has been shown.[1–14] This facile C–H bond scission clearly demonstrates the importance of the neighbouring metal centres for the activation of an inert bond; thus, the formation of a μ–pyridyl group on multimetallic sites is a typical example of multimetallic activation. The μ-pyridyl species is also formed on metal surfaces, such as Pt(111), Ni(100), and Rh(111).[15–20] Although μ-pyridyl complexes are likely important in relation to selective functionalisation of pyridine at the 2-position, their reactivities have scarcely been investigated despite of the abundant reports on their syntheses.

Ellman and co-workers established that a mononuclear Rh/PCy$_3$ system catalyses *ortho*-alkylation and arylation of pyridine via the formation of a *N*-heterocyclic carbene (NHC) intermediate through ortho C–H bond activation of pyridine.[21,22] However, catalysis using a cluster compound is only known for acylation of pyridine by Ru$_3$(CO)$_{12}$.[23]

Scheme 1. Reaction of **1** with 4-methoxypyridine.

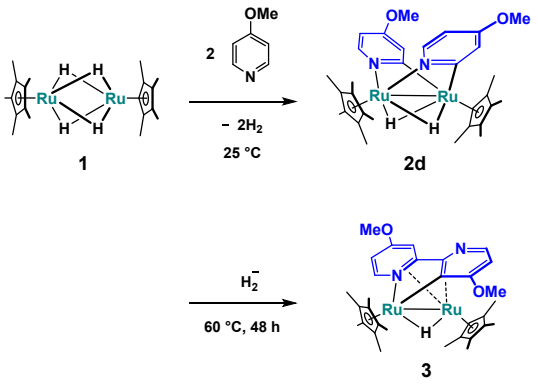

We previously reported dehydrogenative coupling of 4-substituted pyridines catalysed by diruthenium complexes, Cp*Ru(μ-H)$_4$RuCp* (**1**) (Cp* = η^5-C$_5$Me$_5$) and (Cp*Ru)$_2$(μ-H)(μ-PMe$_2$)(μ-η^2:η^2-C$_6$H$_6$),[24] and trinuclear complexes, {Cp*Ru(μ-H)}$_3$(μ$_3$-H)$_2$[25] and (Cp*Ru)$_2$(Cp*Co)(H)$_4$.[26] These reactions likely proceed via the formation of μ- or μ$_3$-pyridyl intermediates. Although complex **1** provides 4,4′-dimethoxy-2,2′-bipyridine in a quite low yield (6%), we obtained bis(μ-pyridyl) complex **2d** by the reaction of **1** with 4-methoxypyridine at 25 °C (Scheme 1). The X-ray diffraction (XRD) study clearly showed that the two pyridyl moieties in **2d** are coordinated to the diruthenium centre in a *cis* geometry and that both nitrogen atoms of the μ-pyridyl ligands are bound to the same ruthenium centre, i.e., they adopt a head-to-head configuration.[24] This structure implies that 2,2′-bipyridine is formed by the reductive C–C bond

Department of Chemical Science and Engineering, School of Materials and Chemical Technology, Tokyo Institute of Technology, 2-12-1 O-okayama, Meguro-ku, Tokyo 152-8552, Japan.

Electronic Supplementary Information (ESI) available: [details of any supplementary information available should be included here]. See DOI: 10.1039/x0xx00000x

formation between the two pyridyl moieties. In fact, we reported that reductive C–C bond formation occurs upon heating in a previous paper.[26] However, instead of the formation of bipyridine, μ-κ(*C*,*N*)-2,2′-bipyrid-3-yl complex **3** is formed via the C–H bond cleavage at the next position of the methoxy group. Therefore, the mechanism of bipyridine formation at the Ru_2 site is still unclear. Moreover, it is also unclear how the formed bipyridine, which often acts as a strong chelating ligand, is liberated from the Ru_2 site.

Herein, we report the results of stoichiometric reactions of **1** with 4-substituted pyridines leading to the formation of novel diruthenium complexes that contains a partially hydrogenated bipyridine ligand and their transformations to μ-η^2:η^2-bipyridine complexes. Their reactivities allow us to propose a plausible mechanism for bipyridine formation at the diruthenium site.

Experimental

General Procedures

All compounds were manipulated using standard Schlenk and high-vacuum-line techniques under an atmosphere of argon. Dehydrated toluene, heptane, hexane, pentane, and tetrahydrofuran (THF), and methanol used in this study were purchased from Kanto Chemicals and stored under an atmosphere of argon. Acetone-d_6 was dried over molecular sieves 3A and stored under an atmosphere of argon. Diethyl ether, benzene-d_6, toluene-d_8, and tetrahydrofuran-d_8 were dried over sodium-benzophenone ketyl and stored under an atmosphere of argon. Cp*Ru(μ-H)$_4$RuCp* (**1**) (Cp* = η^5-C_5Me_5) was prepared according to the previously published method.[27] ^{1}H, ^{13}C, and ^{19}F NMR spectra were recorded on Varian INOVA-400 and Varian 400MR spectrometers. ^{1}H NMR spectra were referenced to tetramethylsilane as an internal standard. ^{13}C NMR spectra were referenced to the natural-abundance carbon signal of the solvent employed. ^{19}F NMR spectra were referenced to external $CFCl_3$. IR spectra were recorded on a JASCO FT/IR-4200 spectrophotometer. Spectral data of each compound are given in Supplementary Information. Elemental analyses were performed on a Perkin Elmer 2400II CHN analyser.

X-ray Diffraction Studies

Single crystals of **4a**, **5c**, **6b**, **7a**, and **8** for the X-ray analyses were obtained directly from the preparations described below and mounted on nylon Cryoloops with Paratone-N (Hampton Research corp.). Diffraction experiments were performed on a Rigaku R-AXIS RAPID imaging plate diffractometer with graphite-monochromated Mo-Kα radiation (λ = 0.71069 Å). Cell refinement and data reduction were performed using the PROCESS-AUTO program.[28] Intensity data were corrected for Lorentz-polarisation effects and empirical absorption. The structures were solved by the direct method using SHELXT-2014/5 and further refined with the SHELXL-2016/6 program package.[29,30] All non-hydrogen atoms were found by the difference Fourier synthesis and were refined anisotropically except for the disordered carbon atoms, C(4), C(5), C(4A), and C(5A), in the dihydrobipyridine group in **5c**. The refinement was carried out by least-squares methods based on F^2 with all measured reflections. The metal-bound hydrogen atoms in **4a** and **8** were located in the difference Fourier map and refined isotropically. Crystal data and results of the analyses are listed in Table S1 in the Supplementary Information. The CIF data is deposited in the Cambridge Crystallographic Data Centre with the deposition numbers of 1901042 (**4a**), 1901043 (**5c**), 1901044 (**6b**), 1901045 (**7a**), and 1901046 (**8**).

Variable Temperature NMR studies and NMR simulation

NMR simulations for the methylene protons of **4a**, **5a**, **5b**, **5c**, **6a**, and **6b** were performed using the gNMR v5.0.6.0 software package (2006, Ivory Soft). Final simulated line shapes were obtained via an iterative parameter search upon the coupling constants among the methylene protons. Complete details of the fitting procedure and results are shown in the Supplementary Information. Variable-temperature NMR studies were performed in NMR tubes equipped with a J. Young valve using a Varian INOVA-400 Fourier transform spectrometer. The NMR simulation for the temperature-dependent signals of **8** was also performed using the gNMR v5.0.6.0 software package via an iterative parameter search upon the exchange constants, *k*, which was the rates for the site exchange of the two Cp* groups. The activation parameters, $\Delta H^{\ddagger}$ and $\Delta S^{\ddagger}$, were determined from the plot of ln(*k*/T) versus 1/T. Estimated standard deviations (σ) in the slope and y intercept of the Eyring plot determined the error in $\Delta H^{\ddagger}$ and $\Delta S^{\ddagger}$, respectively. The standard deviation in $\Delta G^{\ddagger}$ was determined from the formula: $\sigma(\Delta G^{\ddagger})^2 = \sigma(\Delta H^{\ddagger})^2 + [T\sigma(\Delta S^{\ddagger})]^2 - 2T\sigma(\Delta H^{\ddagger})\,\sigma(\Delta S^{\ddagger})$.

Preparations of compounds

(Cp*Ru)$_2${μ-η^2-4,4′-Me$_2$dhbpy}(μ-H)(H) (4a). A 50 mL Schlenk tube was charged with **1** (0.117 g, 0.245 mmol) and THF (10 mL). After 4-picoline (0.25 mL, 2.50 mmol) was added to the solution, the reaction mixture was stirred at 25 °C for 16 h. The colour of the solution turned from red to orange. THF and remaining 4-picoline were removed under reduced pressure. The ^{1}H NMR spectrum of the residual solid revealed that **1** was fully consumed and **4a** and **5a** were formed in 90 and 10% yields, respectively. Analytically pure **4a** was obtained from the diethyl ether solution of the mixture stored at 2 °C as a red single crystal. Anal. Calcd for $C_{32}H_{46}N_2Ru_2$: C, 58.16; H, 7.02; N, 4.24. Found: C, 58.35; H, 7.21; N, 3.89.

(Cp*Ru)$_2${μ-η^4-4,4′-Me$_2$dhbpy} (5a). A 20 mL glass tube equipped with a Teflon valve was charged with **1** (0.105 g, 0.221 mmol) and THF (10 mL). After γ-picoline (0.22 mL, 2.21 mmol) was added to the flask, the solution was stirred at 80 °C for 84 h. The colour of the solution turned from red to reddish-brown. The solvent and remaining 4-picoline were removed under reduced pressure. The ^{1}H NMR spectrum of the residual solid revealed that all of **1** was exclusively converted to **5a**. Anal. Calcd for $C_{32}H_{44}N_2Ru_2$: C, 58.34; H, 6.73; N, 4.25. Found: C, 58.33; H, 6.60; N, 4.14.

The reaction of 1 with γ-picoline in an NMR tube: Formation of {Cp*Ru(μ-4-MeC$_5$H$_3$N)(μ-H)}$_2$ (2a). An NMR tube equipped with a Teflon valve was charged with **1** (6.2 mg, 13 μmol) and benzene-d_6 (0.5 mL) together with ferrocene (4.3 mg, 23 μmol) as an internal standard. After γ-picoline (12 μL, 0.12 mmol) was added to the solution, the NMR tube was kept at 25 °C. The solution was periodically monitored by ^{1}H NMR spectroscopy. The ^{1}H NMR spectrum recorded after 5 min showed that **2a** was formed in 20% yield. The concentration of **2a** then gradually decreased and all of **2a** was consumed after 70 h. The ^{1}H NMR spectrum recorded after 200 h showed that **4a** and **5a** were formed in 45 and 54% yields, respectively.

(Cp*Ru)$_2${μ-η^4-4,4′-(CF$_3$)$_2$dhbpy} (5b). A 50 mL Schlenk tube was charged with **1** (0.344 g, 0.721 mmol) and THF (25 mL). After 4-trifluoromethylpyridine (0.27 mL, 2.33 mmol) was added to the solution, the reaction mixture was stirred at 25 °C for 66 h. The colour of the solution turned from red to dark-brown. Removal of volatiles under reduced pressure afforded an oily residue. The remaining 4-trifluoromethylpyridine was removed under reduced pressure from the residue through azeotropy by the use of heptane. The product was extracted from the residue with 5 mL of hexane three times. The combined extracts were filtered with a glass frit (G4). Removal of the solvent under reduced pressure gave **5b** (0.523 g, 0.683 mmol, 95%). Analytically pure **5b** was obtained as black crystals from the acetone solution stored at −30 °C (0.458 g, 0.598 mmol, 83%). Anal. Calcd for $C_{32}H_{38}F_6N_2Ru_2$: C, 50.12; H, 5.00; N, 3.65. Found: C, 50.37; H, 5.11; N, 3.64.

(Cp*Ru)$_2${μ-η^4-4,4′-(COOEt)$_2$dhbpy} (5c). A 50 mL Schlenk tube was charged with **1** (0.133 g, 0.279 mmol) and THF (10 mL). After ethyl isonicotinate (0.12 mL, 0.881 mmol) was added to the solution, the reaction mixture was stirred at 25 °C for 20 h. The colour of the solution turned from red to brown. Removal of volatiles under reduced pressure afforded a wet residue containing **5c** and unremoved ethyl isonicotinate. The ^{1}H NMR spectra of the residue showed exclusive formation of **5c**. The residue was then dissolved into 15 mL of methanol. Dark brown crystals of **5c** was obtained from the methanol solution stored at −30 °C (92.1 mg, 0.118 mmol, 42%). A brown single crystal used for the diffraction studies was prepared from the cold pentane solution of **5c** stored at −20 °C. Anal. Calcd for $C_{36}H_{48}N_2O_4Ru_2$: C, 55.80; H, 6.24; N, 3.62. Found: C, 55.47; H, 6.22; N, 3.59.

Hydrogenation of 5; formation of (Cp*Ru)$_2${μ-η^2-4,4′-R$_2$dhbpy}(μ-H)(H) (4b, R = CF$_3$; 4c, R = COOEt). An NMR tube equipped with a Teflon valve was charged with **5b** (14.7 mg, 19.2 μmol), benzene-d_6 (0.4 mL), and 2,2,4,4-tetramethylpentane as an internal standard. After the NMR tube was evacuated with a dry ice/methanol bath, 1 atm of dihydrogen was introduced. The tube was then heated at 40 °C, and periodically monitored by ^{1}H NMR spectroscopy. Complex **5b** was gradually converted to **4b**, and the population of **4b** became steady in 24 h, where the **5b**/**4b** ratio was measured at *ca.* 3/1. All of **4b** was immediately converted in **5b** upon heating at 60 °C. Similar reaction occurred with **5c**, however the **5c**/**4c** ratio reached *ca.* 2/1 in 24 h.

(Cp*Ru)$_2$(μ-η^4-4,4′-Me$_2$dhbpy)(^{t}BuNC) (6a). A 50 mL Schlenk tube was charged with **5a** (17.6 mg, 26.7 μmol) and toluene (3 mL). After ^{t}BuNC (30 μL, 0.27 mmol) was added to the solution, the reaction mixture was stirred at 25 °C for 20 min. The colour of the solution did not change from brown. Removal of volatiles under reduced pressure afforded an oily residue. Because **6a** was well soluble to common organic solvents, **6a** could not be recrystallized from the mixture. Although **6a** was not obtained as an analytically pure form, the ^{1}H and ^{13}C NMR spectra of the crude mixture showed that **6a** was formed as a major product in the reaction.

(Cp*Ru)$_2${μ-η^4-4,4′-(CF$_3$)$_2$dhbpy}(^{t}BuNC) (6b). A 50 mL Schlenk tube was charged with **5b** (54.8 mg, 71.5 μmol) and toluene (3 mL). After ^{t}BuNC (0.11 mL, 0.96 mmol) was added to the solution, the reaction mixture was stirred at 25 °C for 1 h. The colour of the solution did not change from brown. Removal of volatiles under reduced pressure afforded an oily brown residue. The remaining toluene was removed under reduced pressure from the residue through azeotropy by the use of pentane. The product was extracted from the residue with 5 mL of pentane three times and the combined extracts were filtered with a glass frit (G4). Removal of the solvent under reduced pressure gave **6b** (41.4 mg, 48.7 μmol, 68%). A brown single crystal of **6b** used for diffraction studies was obtained from the hexane solution stored at −30 °C. Anal. Calcd for $C_{37}H_{47}F_6N_3Ru_2$: C, 52.29; H, 5.57; N, 4.94. Found: C, 52.34; H, 5.68; N, 5.13.

(Cp*Ru)$_2$(μ-η^4-4,4′-Me$_2$bpy) (7a). A 50 mL glass tube equipped with a Teflon valve was charged with **5a** (133.7 mg, 0.203 mmol) and heptane (10 mL). After the tube was evacuated using a liquid N_2 bath, the solution was heated at 140 °C for 38 h. The colour of the solution turned from red to reddish-brown. Removal of the solvents under reduced pressure afforded a black residue including **7a**. The product was extracted from the residue with 5 mL of hexane three times and the combined extracts were condensed to *ca.* 3 mL under reduced pressure. Complex **7a** was obtained as a brown crystalline solid from the hexane solution stored at −30 °C (60.4 mg, 92.0 μmol, 45%). Anal. Calcd for $C_{32}H_{42}N_2Ru_2$: C, 58.52; H, 6.45; N, 4.26. Found: C, 58.04; H, 6.59; N, 4.00. Due to impurities that cannot be separated, the results of carbon analysis were slightly off the calculated value.

Thermolysis of 5b. A 50 mL glass tube equipped with a Teflon valve was charged with **5b** (156.1 mg, 0.204 mmol) and heptane (10 mL). After the tube was evacuated using a liquid N_2 bath, the solution was heated at 140 °C for 6 days. Removal of the solvents under reduced pressure afforded a black residue including **7b**. ^{1}H NMR spectrum of the residue showed the formation of μ-η^2:η^2-bpy complex **7b**, however *ca.* 10% of **5b** still remained. In addition, formation of a small amount of unidentified products was observed. Complex **7b** could not be isolated from the mixture by column chromatography and by recrystallization.

(Cp*Ru)$_2$(μ-η^2-phen)(μ-H)(H) (8). A 50 mL Schlenk tube was charged with **1** (40.1 mg, 84.1 μmol) and THF (20 mL). After 1,10-phenanthroline (20.0 mg, 0.111 mmol) was added to the solution, the reaction mixture was stirred at 40 °C for 48 h. The colour of the solution turned from red to brown. Removal of volatiles under reduced pressure afforded an oily residue containing **8** and unreacted 1,10-phenanthroline. After the residue was rinsed with 5 mL of acetonitrile three times, the residue was dissolved in ca. 2 mL of THF. Complex **8** was obtained as a black single crystal by recrystallization from the cold hexane solution stored at −30 °C. (15.2 mg, 23.2 μmol, 21%). Anal. Calcd for $C_{32}H_{40}N_2Ru_2$: C, 58.70; H, 6.16, N; 4.28. Found. C, 58.66, H, 6.32, N, 4.29.

Reaction of 1 with 4,4′-dimethyl-2,2′-bipyridine. An NMR tube equipped with a Teflon valve was charged with **1** (5.0 mg, 10.5 μmol), 4,4′-dimethyl-2,2′-bipyridine (1.9 mg, 10.3 μmol), and benzene-d_6 (0.4 mL). The tube was then heated at 80 °C and periodically monitored by ^{1}H NMR spectroscopy. The ^{1}H NMR spectrum recorded after 48 h showed that all of **1** was consumed and **5a** and **7a** were formed nearly quantitatively in a ratio of *ca.* 10:1.

Results and discussion

Synthesis of dihydrobipyridine complexes

In contrast to the formation of **3**, the reaction of **1** with γ-picoline proceeded even at 25 °C, and a mixture of two

dinuclear complexes, **4a** and **5a**, was obtained as a consequence of C–C bond formation (Scheme 2). Because of the lack of directing group, a pyridyl-pyridine ligand was not formed, however it was not a bipyridine ligand; one of the pyridine ring was partially hydrogenated, and a dihydrobipyridine (dhbpy) ligand was formed at the Ru_2 site. Complex **5a** is solely obtained in the reaction performed at 80 °C, and treatment of **5a** with 1 atm of H_2 results in the formation of **4a**. These results indicate that **5a** is formed consecutively via the elimination of dihydrogen from **4a**.

Scheme 2. The reaction of 1 with γ-picoline.

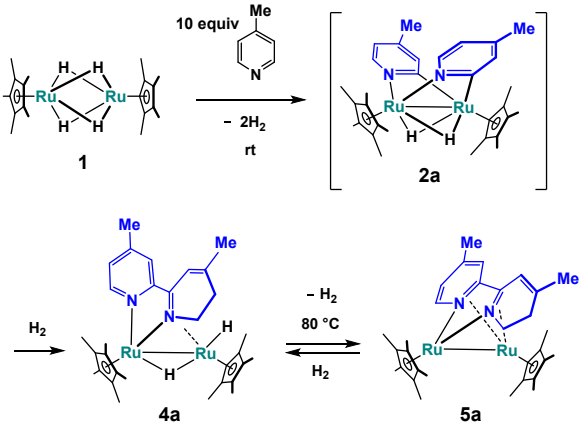

The presence of a dhbpy ligand was clearly confirmed by XRD, as shown in Fig. 1. The molecular structure of **4a** shows that two six-membered rings are connected through the C(1) and C(7) atoms. The formation of **4a** indicates that the C–C bond formation between the two pyridyl moieties occurs even at ambient temperature.

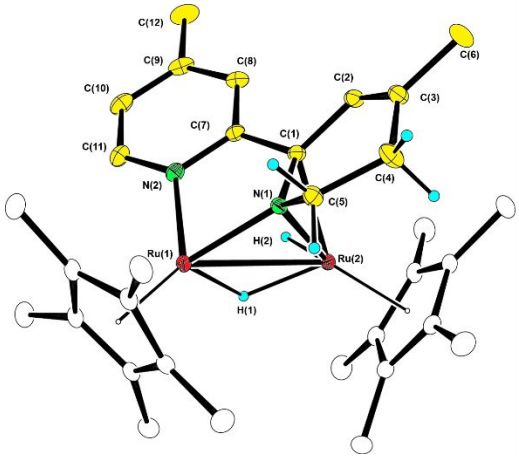

Fig. 1. Molecular structure and labelling scheme of **4a** with thermal ellipsoids at a 40% probability.

Although examples are limited, the stoichiometric formation of 2,2′-bipyridine using a transition metal complex is known. Shibata *et al*. reported the coupling reaction of 2-arylpyridines using a diyttrium complex that has a diamido ligand.[31] Riera and Pérez also reported the formation of a 2,2′-bipyridine ligand upon deprotonation/oxidation of $[fac\text{-}Re(CO)_3(4\text{-}NC_5H_4OMe)_3]^+$.[32] Coupling reactions between two pyridine ligands via direct C–H bond cleavage using Sc,[33] Zr,[34] Ta,[35] and Ru[36] complexes have also been reported. These reactions selectively afford a 2,2′-bipyridine ligand; however, the extraction of the 2,2′-bipyridine ligand from a metal centre has rarely been investigated.[31] Unlike the above-mentioned bipyridine formations, coupling of the two pyridyl moieties at the diruthenium site of **1** occurs with the partial hydrogenation of one pyridine ring to form a dhbpy ligand. While the pyridine moiety is coordinated to Ru(1) only through the N(2) atom, the hydrogenated pyridine ring is π-bonded to Ru(2) with the C(1)=N(1) bond in addition to κ(*N*)-coordination to the Ru(1) atom. The C(1)=N(1) bond (1.4168(19) Å) is significantly elongated owing to the π-coordination compared to the uncoordinated C(7)=N(2) bond (1.363(2) Å). The sum of the bond angles around the C(1) atom is ca. 351°, which shows the loss of planarity at this position. Consequently, the two six-membered rings are no longer coplanar and are folded at the C(1) atom.

In the ^{13}C NMR spectrum of **4a**, two singlet signals that were assigned to the diazaruthenacycle moiety were observed at δ 173.4 and 62.6 ppm. Because the former singlet is typical for the α-carbon signal of pyridine, this was assigned to the signal of the C(7) atom. In contrast, the C(1) atom is shielded substantially owing to the π-coordination to the Ru(2) atom and thus underwent a significant upfield shift.

The methylene protons at the C(5) atom resonate at δ 3.84 and 4.52 ppm as multiplets with a large geminal coupling constant (J_{HH} = 13.2 Hz), whereas those at the C(4) atom should resonate at δ 1.6 and 1.9 ppm based on the correlation with the ^{13}C signal of the C(4) atom (δ 29.8). However, they were not clearly observed owing to the obstruction by the intense Cp* and methyl signals.

The positions of the two hydrido ligands in **4a** were successfully determined by XRD. The H(1) atom bridges the two metal centres, and the H(2) atom is bonded to the Ru(2) atom as a terminal hydride. The presence of a terminal hydride was also determined by the IR spectrum, which showed a sharp ν(Ru–H) absorption at 1986 cm^{-1}. This absorption disappeared in **5a** owing to lack of hydrido ligands.

Because there were unresolved disordered structures in the dhbpy moiety, we could not refine the structure of **5a** by XRD. Nevertheless, the preliminary result suggests μ-η^4-coordination of the dhbpy ligand as shown in Fig. S39 in the Supplementary Information. The coordination mode of the dhbpy ligand was eventually confirmed in **5c**, which was obtained by the reaction of **1** with ethyl isonicotinate (*vide infra*).

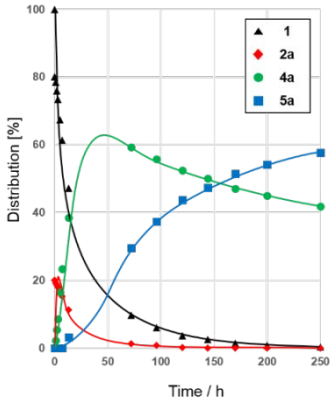

Fig. 2. Time course of reaction of **1** with γ-picoline at 25 °C in C_6D_6.

π-Coordination of both C=N bonds in the dhbpy moiety to the Ru(2) atom was also clearly demonstrated by the upfield shift of the ^{13}C signals of the diazaruthenacycle moiety (δ 91.5 and 101.2 ppm). The μ-η^4-coordination means that the dhbpy ligand in **5a** acted as an 8-electron donor, which compensated for the lack of electrons owing to the dihydrogen elimination, and this caused **5a** to be coordinatively saturated. Similar transformation of the 1,4-diazabutadiene ligand from μ-η^2- to the μ-η^4-mode accompanied by the loss of the CO ligand in Ru_2(μ-RN=CH–CH=NR-)$(CO)_6$, has been well documented by van Koten and co-workers.[37]

During the initial stage of the reaction, another hydrido signal was observed at δ −9.33 ppm prior to the formation of **4a**. Based on the similarity of the chemical shift to the hydride of **2d** (δ −9.24),[24] we assume that this species is bis(μ-picolyl) complex **2a**. The time course of the reaction showed that initial product **2a** was converted to **4a** and then transformed successively consecutively into **5a** (Fig. 2).

Scheme 3. Plausible mechanism for the formation of **4a**.

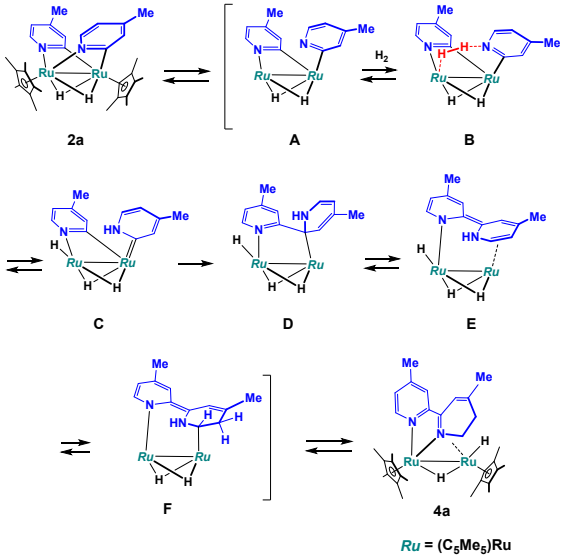

One plausible mechanism for formation of the dhbpy ligand is shown in Scheme 3. Complex **2a** is required to uptake one dihydrogen molecule to form **4a**, whereas **2a** is coordinatively saturated. Thus, a vacant site should be generated on **2a**, likely by decoordination of the nitrogen atom, leading to the formation of the κ(*C*)-pyridyl intermediate, **A**. Although formation of a κ(*C*)-pyridyl ligand at a multinuclear site has never been reported, transformation of a κ(*N*)-pyridine ligand into a κ(*C*)-pyridyl or an NHC ligand has been often observed for mononuclear complexes.[38–41] As mentioned later, the μ-1,10-phenanthroline (phen) ligand in **8** is inferred to show similar motion.

Unsaturated intermediate **A** can uptake dihydrogen, which is accumulated in the reaction vessel by the formation of **2a**. Although the population of **2a** gradually decreased, as shown in Fig. 2, introduction of H_2 into the tube resulted in immediate conversion of **2a** to **4a**. This rapid H_2 incorporation suggests a mechanism that involves heterolytic H–H bond cleavage, leading to the formation of the NHC intermediate, **C** (Scheme 3). The NHC ligand in **C** inserts into the Ru–C bond to form **D**. π-Coordination of the C=C bond to Ru(2), followed by the insertion into a Ru–H bond, explains the hydrogenation at the C(4)–C(5) position. Migration of the NH proton to the metal centre accompanied by aromatisation at the pyridine moiety forms the dhbpy ligand. The crucial role of the hydrogen bond in the formation of the NHC ligand has been documented by the Carmona's and Estruelas's groups.[40,41]

Notably, the catalysis by **1** must be conducted in a sealed vessel, although this is a dehydrogenative coupling of pyridines. When the reaction was conducted in an open vessel under an Ar atmosphere, no bipyridine was formed. Decomposition of the catalyst was only observed in the open vessel. This result also implies the necessity of dihydrogen for C–C bond formation.

Scheme 4. The reaction of **1** with pyridines containing an electron-withdrawing group at the 4-position.

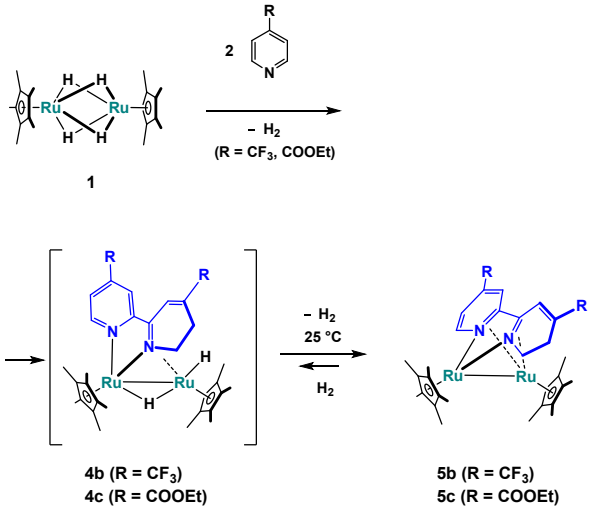

Complex **4a** gradually converted to **5a** at 25 °C; however, the conversion accelerated upon heating. The reaction of **1** with pyridines containing an electron-withdrawing group at the 4-position proceeded similarly; however, **5** was exclusively obtained even at 25 °C (Scheme 4). Because of the low-lying π*(C=N) orbital, π-coordination of the C=N bond of the pyridine moiety was promoted, which effectively extruded dihydrogen from **4**. When **5b** was treated with dihydrogen in a sealed NMR tube, two doublets stemmed from the hydrido ligands of **4b** began to appear at δ −14.89 and −11.26 (J_{HH} = 5.1 Hz). However, even under an H_2 atmosphere, the population of **4b** did not exceed above 25%. This result suggests that **5b** equilibrates with **4b**. Treatment of **5c** with 1 atm of H_2 also afforded **4c**, and the **4c** ratio was estimated to be 33%. Complexes **4b** and **4c** were readily converted to **5b** and **5c**, respectively, by removing dihydrogen from the NMR tube or upon heating above 60 °C under an H_2 atmosphere.

The molecular structure of **5c** was determined by XRD, as shown in Fig. 3. There is a crystallographic mirror plane passing through the Ru(1)–Ru(2) vector and the centre of the two six-membered rings. Consequently, the two six-membered rings, the pyridine and dihydropyridine moieties, were disordered. Although a precise discussion about the bond distances in the dhbpy ligand is not plausible, π-coordination of both C=N bonds to the Ru(2) atom was clearly observed; the C(1)=N(1) distance

(1.405(2) Å) is comparable to the π-coordinated C=N distance in **4a** (1.4168(19) Å).

While the C(1)–C(1#) distance (1.425(3) Å) is slightly larger than those reported for μ-diimine ligands (1.347–1.420 Å),[37,42–46] this is considerably shorter than that of the uncoordinated diethyl 2,2′-bipyridine-4,4′-dicarboxylate (1.492 Å).[47] The long C=N bonds and short C–C bond indicate the substantial back donation from Ru(2) to the LUMO of the diimine moiety, which has bonding character between the two central C atoms and is antibonding between the C and N atoms.[37]

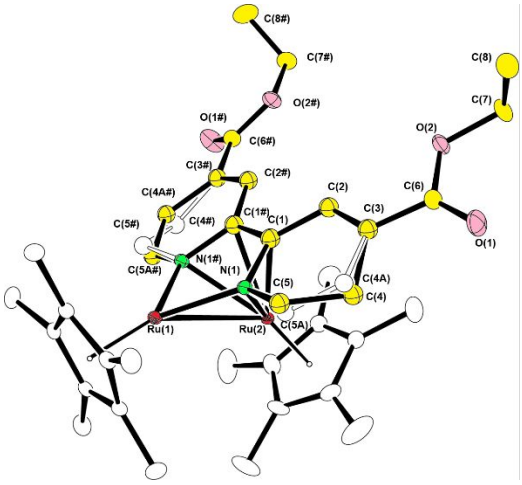

Fig. 3. Molecular structure and labelling scheme of **5c** with thermal ellipsoids at a 30% probability.

Reactivity of μ-η⁴-dhbpy complex 5

Scheme 5. Reactivity of μ-η²:η²-dhbpy complex **5**.

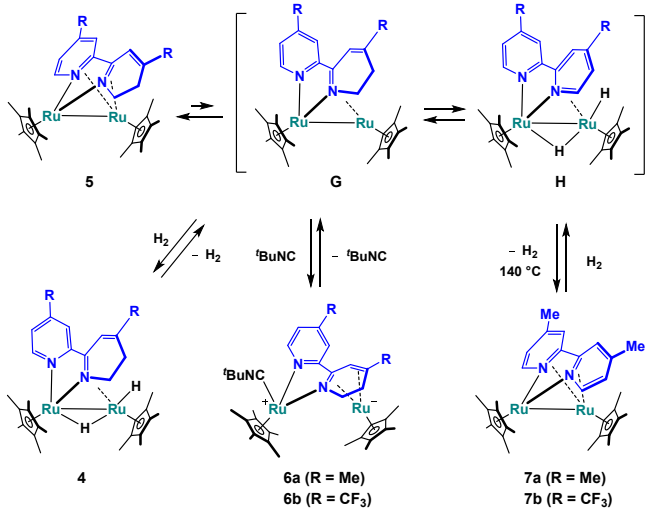

Because of the μ-η⁴-coordination of the dhbpy moiety, complex **5** adopted a coordinatively saturated 34-electron configuration. Nevertheless, **5** readily reacted with dihydrogen to yield dihydrido complex **4**, as mentioned above. This suggests that the π-coordination of the pyridine ring is weak and a vacant site would be generated by the decoordination of the pyridine moiety. This led to the formation of **G** shown in Scheme 5, which possesses a μ-η²-coordinated dhbpy ligand. Notably, this resulted in the resonance stabilisation of the pyridine moiety in **G**, which may antagonise the destabilisation derived from the formation of a vacant site. van Koten and Vrieze also noted that the diazabutadiene ligand in $Ru_2(\mu\text{-}\eta^4\text{-RN=CH–CH=NR-})(CO)_5$ lies in equilibrium between the 8- and 6-electron coordination modes in solution[37] in which the μ-diazabutadiene complex reacts with dihydrogen to yield a dihydrido complex that has a μ-η²-diazabutadiene ligand.[48]

To verify the flexibility of the dhbpy ligand in **5**, the reaction of **5** with ^{t}BuNC was examined (Scheme 5). Although the product in the reaction of **5a** with ^{t}BuNC could not be isolated owing to its high solubility toward common organic solvents, complex **6b**, which was obtained by the reaction of **5b**, was isolated in an analytically pure form. The XRD study of **6b** revealed that the dhbpy ligand adopted a μ-η⁴-coordination mode, as depicted in Fig. 4.

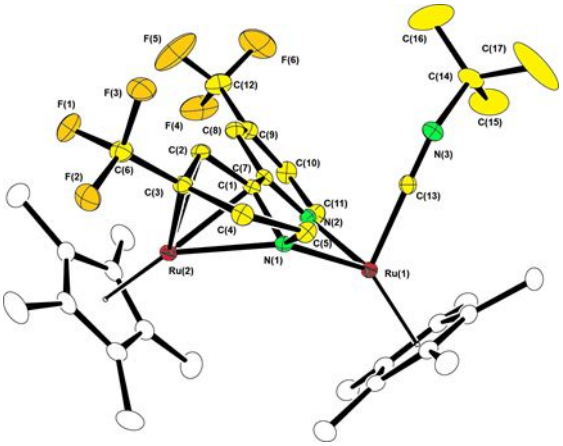

Fig. 4. Molecular structure and labelling scheme of **6b** with thermal ellipsoids at a 30% probability.

While both nitrogen atoms of the dhbpy ligand were bound to the Ru(1) atom to which ^{t}BuNC was coordinated, the dhbpy moiety was coordinated to the Ru(2) atom in an η⁴-fashion as an azadiene. The interatomic distance between the Ru(1) and Ru(2) atoms (4.13 Å) clearly showed that there was no direct bonding interaction between them.

Because **6** is diamagnetic, the formal oxidation states of the Ru(1) and Ru(2) atoms should be +2 and 0, respectively. This suggests that Ru(1) is monocationically charged, which makes the Ru(1) centre coordinatively saturated. Consequently, this resulted in the rupture of the Ru–Ru bond. The liberated $[Cp^*Ru]^-$ moiety was then arrested by the dhbpy ring, where the η⁴-coordination of the dhbpy moiety also made the Ru(2) atom coordinatively saturated.

The η⁴-coordination of the azadiene moiety was also determined by the remarkable upfield shift of the ^{13}C NMR signals. The ^{13}C signals that originated from the carbon atoms at the 3- and 4-positions of the dhbpy ring in **5a** (δ 116.3 and 131.2 ppm) shift to δ 71.5 and 59.7 ppm in **6a**. In **6b**, these signals underwent a further upfield shift to δ 35.0 and 54.5 ppm.

Thermolysis of **6a** resulted in the regeneration of **5a** via the decoordination of ^{t}BuNC accompanied by the reconstruction of a Ru–Ru bond. As shown in the transformations between **4**, **5**, and **6**, the dhbpy ligand varied its coordination mode readily in response to the electron configuration at the metal centres.

The products of the catalysis were bipyridines; therefore, dehydrogenation from the dhbpy ligand should be involved in the catalytic cycle. In fact, μ-η²:η²-bipyridine complex **7a** was

obtained upon thermolysis of **5a** at 140 °C under reduced pressure.

Dehydrogenation of the dhbpy ligand in **5a** likely proceeds via oxidative addition of the C–H bond adjacent to the nitrogen atom. This process requires generation of a vacant site; thus, C–H bond cleavage also likely occurs in intermediate **G**, as shown in Scheme 5. C–H bond cleavage of amine at the α-position has been shown to readily occur at a multinuclear site.[49, 50] The bipyridine intermediate, **H**, which has two hydrides, is formed via the following β-hydrogen elimination. As described later, a model complex of **H** was obtained by the reaction of **1** with 1,10-phenanthroline. The subsequent reductive elimination of dihydrogen from **H** afforded **7a**. As seen in the dhbpy ligand in **4a**, the decrease in the valence electrons, which originated from the H_2 elimination, was compensated for by the μ-η^2:η^2-coordination of the bipyridine ligand. The molecular structure of **7a** was determined by XRD (Fig. 5). The structural parameters of **7a** were very similar to those of **5c** except for differences arising from the dihydropyridine ring.

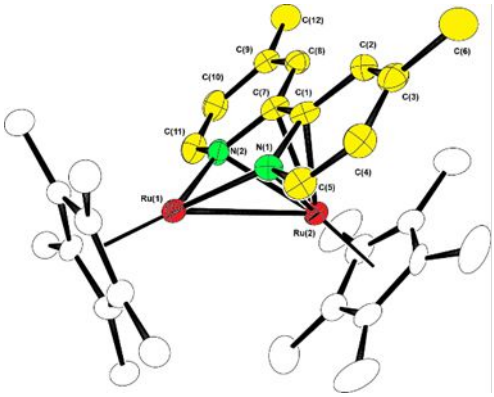

Fig. 5. Molecular structure and labelling scheme of **7a** with thermal ellipsoids at a 40% probability.

Complex **7a** was hydrogenated at 25 °C to regenerate **5a** and **4a**; treatment of **7a** with 1 atm of H_2 at 25 °C resulted in the formation of a mixture of **4a**, **5a**, and **7a** in a ratio of 52:35:13, respectively, in 100 h. A vacant site for the incorporation of dihydrogen was likely generated in **7a** via decoordination of the C=N bond, like in **5a**.

Thermolysis of **5b** also afforded μ-4,4′-di(trifluoromethyl)-2,2′-bipyridine complex **7b**. However, the reaction rate was extremely slow compared to that of the thermolysis of **5a**; ca. 10% of **5b** remained after 6 days. This was likely due to the electron-withdrawing nature of the CF_3 group, which stabilises the π-coordination of the C=N bond.

Property of a μ- phenanthroline complex 8

Complex **7a** was likely an intermediate in the dehydrogenative coupling of γ-picoline. However, 4,4′dimethyl-2,2′-bipyridine was obtained only in 37% based on **7a** in the reaction of **7a** with γ-picoline at 160 °C. In addition, **4a** and **5a** were not formed in the reaction; only a mixture of unidentified complexes was obtained. This fact strongly implied that bipyridine was formed via the decomposition of **7a**, not via catalysis.

In contrast, when the reaction was conducted under an H_2 atmosphere, 4,4′-dimethyl-2,2′-bipyridine was catalytically formed, where the yield was estimated to be *ca.* 500% based on **7a**. As shown in Scheme 5, μ-bipyridine complex **7a** equilibrated with μ-dhbpy complex **5a** via the incorporation of H_2. As mentioned above, the catalysis must be conducted in the presence of dihydrogen. Considering the crucial role of dihydrogen, intermediate **H** is assumed to be responsible for removal of bipyridine from the dinuclear site.

There are 34 valence electrons in **H** considering that the bipyridine ligand adopts a μ-η^2-coordination mode. This means that intermediate **H** may not have reacted with pyridine. However, a coordinatively unsaturated species can be generated by the motion of the μ-bipyridine ligand, which was inferred by the dynamic behavior of 1,10-phenanthroline complex **8**.

Scheme 6. The reaction of **1** with 1,10-phenanthroline

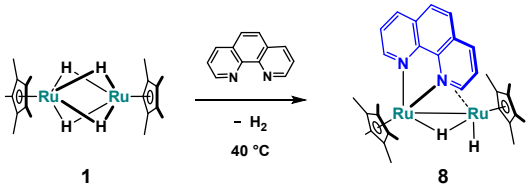

Treatment of **1** with 1,10-phenanthroline at 25 °C resulted in the exclusive formation of μ-phen complex **8** (Scheme 6). Hydrogenation of the aromatic ring did not occur at least up to 60 °C. This was probably due to the rigidity of the phen skeleton compared to that of the bipyridine ligand.

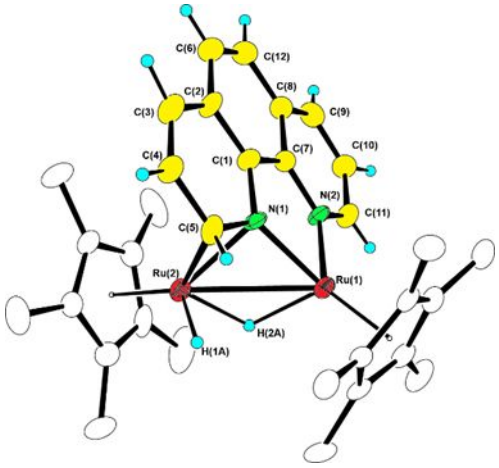

Fig 6. Molecular structure and labelling scheme of **8** with thermal ellipsoids at a 30% probability.

The structure of **8** was determined by XRD. Because there are two independent molecules having similar structural parameters in the unit cell, the structure of only one molecule is shown in Fig. 6. Similar to the dhbpy ligand in **4a**, two nitrogen atoms are coordinated to the same ruthenium centre, Ru(1). Although the position of the π-bonded C=N bond is different from that in **4a**, the phen moiety is attached to the Ru(2) atom via an additional π-coordination through the C(5)=N(1) bond; the Ru(2)–C(5) and Ru(2)–N(1) distances are 2.195(10) and 2.101(8) Å, respectively. Despite the π-coordination of the C(5)=N(1) bond, the phen skeleton still adopts a flat structure; the sum of the bond angles around C(1) and C(7) are 360.0° and

360.1°, respectively. The molecular plane of the phen ligand is diagonal to the Ru(1)–Ru(2) vector by *ca.* 50°.

The ^{13}C signal derived from the π-bonded C=N moiety resonated at δ 63.3 as a doublet (J_{CH} = 181 Hz). Due to the π-coordination to the Ru(2) atom, the signal showed significant upfield shift compared to those of the other ^{13}C signals derived from the phen moiety that were observed in the range between δ 114 and 151 ppm.

In contrast to **4a**, the Cp* group at the Ru(2) atom largely deviates from the Ru–Ru vector; the angle of the centroid of the Cp* group at the Ru(2) atom with the Ru(1)–Ru(2) vector was estimated to be *ca.* 40°. This deviation likely arose from the steric repulsion with the π-bonded ring of the phen moiety, which made the relative positions of the hydrides with respect to the Ru–Ru vector different from those observed in **4a**. Consequently, the Cp* group is located facing the plane of the phen ligand. This arrangement resulted in considerable upfield shift of the Cp* signal in the ^{1}H NMR spectrum, likely owing to the ring current shield; one of the Cp* signals of **8** resonated at δ 1.16 ppm, which is in considerable contrast to the Cp* signals of **4a** that resonate at δ 1.64 and 1.77 ppm.

In the ^{1}H NMR spectrum of **8**, two hydrido signals were observed at δ −13.52 and −13.39 ppm. Although the signal resonating at δ −13.52 was sharp at ambient temperature, the signal resonating at δ −13.39 appeared to be broad (Fig. 7c). The ^{1}H signal derived from the π-bonded C=N moiety that resonated at δ 4.35 also broadened (Fig. 7a). This broadening arose from the site exchange of the hydrogen atom at the C(5) atom with one of the hydrido ligands. Selective irradiation of the signal at δ 4.35 at 25 °C resulted in the complete disappearance of the hydrido signals at δ –13.39, whereas the signal intensity of the other hydrido signal did not change. The observation of spin-saturation-transfer clearly showed that the site exchange occurred via the formation of a μ-κ(*C*)-phenanthrolyl or a μ-NHC intermediate. The variable temperature NMR study combined with the simulation showed that the activation parameters for the site exchange were $\Delta H^{\ddagger}$ = 18.3(3) kcal mol^{-1} and $\Delta S^{\ddagger}$ = 7.1(10) cal mol^{-1} K^{-1}.

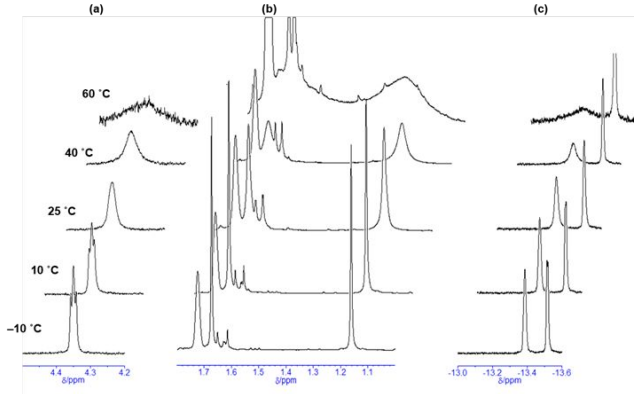

Fig. 7. Variable temperature ^{1}H NMR spectra of **8** showing (a) the methine proton at the η^2-N=CH moiety and the (b) Cp* and (c) hydrido regions (400 MHz, THF-d_8).

With an increase in temperature, two Cp* signals also began to broaden and coalesce into one peak at 70 °C (Fig. 7b). The rates of the site exchange of the Cp* groups were identical to those of the hydrido and the methine proton. These spectral changes are rationalised by the oxidative addition of the C–H bond at the C(5) position, followed by migration of the generated phenanthrolyl group between the two metal centres and leading to the formation of the μ-NHC intermediate, as shown in Scheme 7.

Oxidative addition of the C–H bond at the π-coordinated C=N bond affords μ-phenanthrolyl intermediate **I-1**. Unlike the μ-pyridyl ligand in **2a**, which is parallel to the Ru–Ru vector, the μ-phenanthrolyl group should be diagonal to the Ru–Ru bond because of the steric repulsion with the Cp* groups. This results in the facile transformation of the μ-phenanthrolyl group into a μ-carbene ligand with a hydride migration at the nitrogen atom, as shown in **I-2**. Recently, we reported the synthesis of a related μ-oxycarbene complex and its dynamic behaviour, leading to the rotation of the carbene ligand with respect to the Ru–Ru vector.[51] The μ-NHC ligand would undergo a similar dynamic process, likely via the bridge-to-terminal isomerisation of the carbene ligand. This motion results in the site exchange of the two μ-hydrides in **I-2**, which were originated from the terminal hydride and the methine proton in **8**. Notably, the μ-hydride in **8** only moves to the nitrogen atom and does not participate in the site exchange, which is consistent with the VT-NMR observation.

Scheme 7. Plausible mechanism for the dynamic behaviour of **8**.

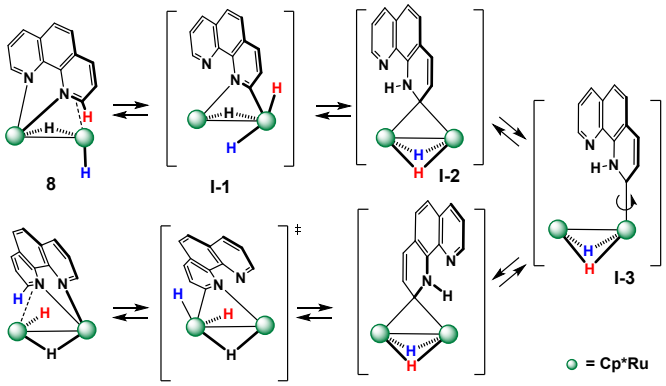

Owing to the detachment of the *N,N*′-chelation, the sum of the valence electrons of the μ-NHC intermediate **I-2** decreased to 30. The *N,N*′-chelation of the phen moiety was not preferred owing to the electrostatic repulsion with the electron rich Ru_2 centre that was composed of strong electron-donating Cp* groups. This propensity of the Ru_2 site derived from **1** enables the transformation of the phen ligand and led to the generation of a vacant site. We previously showed that the μ_3-pyridyl complex isomerised to a face-capping pyridine complex, $\{Cp^*Ru(\mu\text{-}H)\}_3(\mu_3\text{-}\eta^2\text{:}\eta^2\text{:}\eta^2\text{-}C_5H_5N)$.[25]

A similar transformation is expected to occur in the μ-η^2-bpy intermediate **H**, shown in Scheme 5. Owing to its unsaturated nature, the μ-NHC intermediate can react with pyridine, which should be the key-step for the removal of bipyridine from the Ru_2 site.

The reaction of **1** with 4,4′-dimethyl-2,2′-bipyridine was also examined at 80 °C. Although a small amount of **7a** was formed, the reaction mainly afforded **5a** (> 90%). This result indicates that hydrogenation of bipyridine readily occurred at the Ru_2 site, unlike the reaction with 1,10-phenanthroline. This is likely owing to the facile π-coordination of one of the pyridine rings via the rotation around the C–C bond.

In addition, the facile incorporation of 4,4′-dimethyl-2,2′-bipyridine at the Ru_2 site suggests that product inhibition occurs during catalysis. In fact, the initial turnover frequency (TOF) of the dehydrogenative coupling of γ-picoline with 1 mol% of **1** was 4.7 h^{-1}, and the yield of 4,4′-dimethyl-2,2′-bipyridine exceeded 50% within 3 h. However, the yield did not increase further, which was likely because of the product inhibition.

Conclusions

Based on these results, we propose a plausible mechanism for the bipyridine formation by **1**, as shown in Scheme 8. Tetrahydrido complex **1** reacts with two pyridine molecules to yield bis(μ-pyridyl) complex **2**. Complex **2** immediately uptakes dihydrogen to form μ-η^2-dhbpy complex **4** via the coupling of the two μ-pyridyl groups. At elevated temperatures, the hydrides in **4** are removed, and μ-η^2:η^2-dhbpy complex **5** is formed. Decoordination of the η^2-C=N bond of the pyridine moiety in **5**, followed by the C–H bond scissions, affords μ-bpy intermediate **H**. Intermediate **H** isomerises to unsaturated μ-NHC intermediate **I**, as does μ-η^2-phen complex **8**. Intermediate **I** can uptake a third pyridine molecule, which promotes the elimination of bipyridine from the Ru_2 site. The subsequent C–H bond scission at the 2-position of the pyridine ligand regenerates μ-pyridyl intermediate **K**. We showed that **1** catalyses the coupling reaction of pyridines that only contain an electron-donating ligand at the 4-position.[24] As shown in the thermolysis of **5b**, the electron withdrawing substituent makes the generation of a vacant site difficult. In addition, even though **H** was formed, the electron-withdrawing nature of the bpy group promoted the μ-η^4-coordination, leading to the formation of inactive **7**, which caused the decomposition of the dinuclear species.

Scheme 8. Plausible mechanism of bipyridine formation by **1**

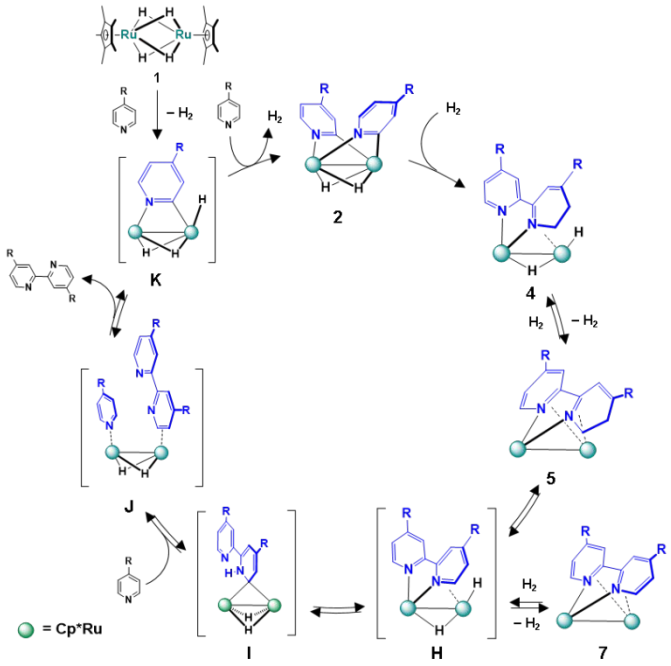

Notably, complex **1** did not react with the 2-substituted pyridines. This was likely owing to the steric repulsion with the Cp* groups. Thus, the C–H bond at the 6-position of 2,2′-bipyridine could not be broken. The steric demand arising from the bulky $(Cp^*Ru)_2$ skeleton suppressed the overreaction of 2,2′-bipyridine, i.e., the formation of terpyridines. This is the most distinctive feature of the catalysis by **1** from catalyses by heterogeneous catalysts, such as Pd/C and Raney-Ni.[52,53]

The other striking feature of the series of reactions is that the coordination mode of the heterocyclic ligands varied at the Ru_2 site in response to the electron configuration. The coordination mode of the dhbpy ligand varied among the μ-η^2-, μ-η^2:η^2-, and μ-η^4-modes. The electron-rich Ru_2 site derived from **1** enabled these facile transformations. We continue to study the properties of the μ-NHC intermediate, which may lead to novel catalysis of heterocyclic compounds via the use of multimetallic complexes.

Conflicts of interest

The authors stated there are no conflicts to declare.

Acknowledgements

The present research was supported by a Grant-in-Aid for Scientific Research in Innovative Areas “Molecular Activation Directed Toward Straightforward Synthesis” from the MEXT of Japan. This work was also partly supported by JST ACT-C Grant Number JPMJCR12YA, Japan.

Notes and references

1 C. C. Yin and A. J. Deeming, *J. Chem. Soc., Dalton Trans.*, 1975, 2091–2096.
2 K. Burgess, B. F. G. Johnson and J. Lewis, *J. Organomet. Chem.*, 1982, **233**, C55–C58.
3 A. J. Deeming, R. Peters, M. B. Hursthouse and J. D. J. Backer-Dirks, *J. Chem. Soc., Dalton Trans.*, 1982, 787–791.
4 A. Eisenstadt, C. M. Giandomenico, M. F. Fredrick, and R. M. Laine, *Organometallics*, 1985, **4**, 2033–2039.
5 G. A. Foulds, B. F. G. Johnson, and J. Lewis, *J. Organomet. Chem.*, 1985, **294**, 123–129.
6 M. I. Bruce, M. G. Humphrey, M. R. Snow, E. R. Tiekink, and R. C. Wallis, *J. Organomet. Chem.*, 1986, **314**, 311–322.
7 C. J. Adams, M. I. Bruce, B. W. Skelton, and A. H. White, *J. Organomet. Chem.*, 1993, **445**, 211–217.
8 T. Beringhelli, G. D’Alfonso, G. Ciani, D. M. Proserpio, and A. Sironi, *Organometallics*, 1993, **12**, 4863–4870.
9 M. P. Cifuentes, M. G. Humphrey, B. W. Skelton, and A. H. White, *J. Organomet. Chem.*, 1994, **466**, 211–220.
10 S. L. Darling, P. K. Y. Goh, N. Bampos, N. Feeder, M. Montalti, L. Prodi, B. F. G. Johnson, and J. K. M. Sanders, *Chem. Commun.*, 1998, 2031–2032.
11 D. R. Gard and T. L. Brown, *Organometallics*, 1982, **1**, 1143–1147.
12 P. O. Nubei, S. R. Wilson, and T. L. Brown, *Organometallics*, 1983, **2**, 515–525.
13 F. A. Cotton and R. Poli, *Organometallics*, 1987, **6**, 1743–1751.
14 F. A. Cotton, C. A. Murillo, and S.-E. Stiriba, *Inorg. Chem. Commun.*, 1999, **2**, 463-464.
15 R. M. Wexler, M.-C. Tsai, C. M. Friend, and E. L. Muetterties, *J. Am. Chem. Soc.*, 1982, **104**, 2034–2036.
16 N. J. DiNardo, P. Avouris, J. E. Demuth, *J. Chem. Phys.*, 1984, **81**, 2169–2180.

17 A. L. Johnson, E. L. Muetterties, J. Stöhr, and F. J. Sette, *Phys. Chem.*, 1985, **89**, 4071–4075.
18 V. H. Grassian and E. L. Muetterties, *J. Phys. Chem.*, 1986, **90**, 5900–5907.
19 C. M. Mate, G. A. Somorjai, H. W. K. Tom, X. D. Zhu, and Y. R. Shen, *J. Chem. Phys.*, 1988, **88**, 441–450.
20 S. Haq and D. A. King, *J. Phys. Chem.*, 1996, **100**, 16957–16965.
21 J. C. Lewis, R. G. Bergman, and J. A. Ellman, *J. Am. Chem. Soc.*, 2007, **129**, 5332–5333.
22 A. M. Berman, J. C. Lewis, R. G. Bergman, and J. A. Ellman, *J. Am. Chem. Soc.*, 2008, **130**, 14926–14927.
23 E. J. Moore, W. R. Pretzer, T. J. O'Connell, J. Harris, L. LaBounty, L. Chou, and S. S. Grimmer, *J. Am. Chem. Soc.*, 1992, **114**, 5888–5890.
24 T. Kawashima, T. Takao, and H. Suzuki, *J. Am. Chem. Soc.*, 2007, **129**, 11006–11007.
25 T. Takao, T. Kawashima, H. Kanda, R. Okamura, and H. Suzuki, *Organometallics*, 2012, **31**, 4817–4831.
26 M. Nagaoka, T. Kawashima, H. Suzuki, T. Takao, *Organometallics*, 2016, **35**, 2348–2360.
27 H. Suzuki, H. Omori, D. H. Lee, Y. Yoshida, M. Fukushima, M. Tanaka, and Y. Moro-oka, *Organometallics*, 1994, **13**, 1129–1146.
28 PROCESS-AUTO: Automatic Data Acquisition and Processing Package for Imaging Plate Diffractometer; Rigaku Corporation: Tokyo, Japan, 2015.
29 G. M. Sheldrick, A*cta Crystallogr., Sect. A: Found. Crystallogr.*, 2015, **A71**, 3–8.
30 G. M. Sheldrick, *Acta Crystallogr., Sect. C: Struct. Chem.*, 2015, **C71**, 3–8.
31 Y. Shibata, H. Nagae, S. Sumiya, R. Rochat, H. Tsurugi, and K. Mashima, *Chem. Sci.*, 2015, **6**, 5394–5399.
32 M. E. Viguri, J. Pérez, L. Riera, *Chem. Eur. J.*, 2014, **20**, 5732–5740.
33 C. T. Carver and P. L. Diaconescu, *J. Am. Chem. Soc.*, 2008, **130**, 7558–7559.
34 G. T. Plubdrich, H. Wadepohl, E. Clot, and L. H. Gade, *Chem. Eur. J.*, 2016, **22**, 9283–92929.
35 H. S. Soo, P. L. Diaconescu, and C. C. Cummins, *Organometallics*, 2004, **23**, 498–503.
36 B. R. Cockerton and A. J. Deeming, *J. Organomet. Chem.*, 1992, **426**, C36–C39.
37 J. Keijsper, L. Polm, G. van Koten, K. Vrieze, G. Abbell, and C. H. Stam, *Inorg. Chem.*, 1984, **23**, 2142–2148.
38 R. Cordone and H. Taube, *J. Am. Chem. Soc.*, 1987, **109**, 8101–8102.
39 H. E. Selnau and J. S. Merola, *Organometallics*, 1993, **12**, 1583–1591.
40 E. Alvarez, S. Conejero, M. Paneque, A. Petronilho, M. L. Poveda, O. Serrano, and E. Carmona, *J. Am. Chem. Soc.*, 2006, **128**, 13060–13061.
41 M. L. Buil, M. A. Esteruelas, K. Gracés, M. Oliván, and E. Oñate, *J. Am. Chem. Soc.*, 2007, **129**, 10998–10999.
42 R. D. Adams, *J. Am. Chem. Soc.*, 1980, **102**, 7476–7479.
43 L. H. Staal, G. van Koten, K. Vrieze, F. Ploeger, and C. H. Stam, *Inorg. Chem.*, 1981, **20**, 1830–1835.
44 P. L. Motz, J. P. Williams, J. J. Alexander, D. M. Ho, J. S. Ricci, and W. T. Miller Jr., *Organometallics*, 1989, **8**, 1523–1533.
45 F. Muller, G. van Koten, K. Vrieze, and D. Heijdenrijk, *Inorg. Chim. Acta*, 1989, **158**, 69–79.
46 R. Abbel, K. Abdur-Rashid, M. Faatz, A. Hadzovic, A. J. Lough, and R. H. Morris, *J. Am. Chem. Soc.*, 2005, **127**, 1870–1882.
47 M. Gembicky, A. Y. Kovalevsky, and P. Coppens, CSD Communication (private communication), CCDC 229910 (2004).
48 J. Keijsper, L. H. Polm, G. van Koten, K. Vrieze, E. Nielsen, and C. H. Stam, *Organometallics*, 1985, **4**, 2006–2012.
49 R. D. Adams, H.-S. Kim, and S. Wang, *J. Am. Chem. Soc.*, 1985, **107**, 6107–6108.
50 R. D. Adams and J. E. Babin, *Organometallics*, 1988, **7**, 963–969.
51 R. Shimogawa, G. Konishi, T. Takao, and H. Suzuki, *Organometallics*, 2016, **35**, 1446–1457.
52 P. E. Rosevear and W. H. F. Sasse, *J. Heterocyclic Chem.*, 1971, **8**, 483–485.
53 G. M. Badger and W. H. F. Sasse, *J. Chem. Soc.* 1956, 616–620.